Magnetic static response functions

2003 J. Phys.: Condens. Matter 15 S617

(http://iopscience.iop.org/0953-8984/15/5/314)

INSTITUTE OF PHYSICS PUBLISHING JOURNAL OF PHYSICS: CONDENSED MATTER

J. Phys.: Condens. Matter **15** (2003) S617–S630 PII: S0953-8984(03)56503-1

Magnetic static response functions

H Ebert, S Mankovskyy, H Freyer and M Deng

Physical Chemistry, University of Munich, Butenandtstrasse 5-13, D-81377 München, Germany

Received 22 November 2002
Published 27 January 2003
Online at stacks.iop.org/JPhysCM/15/S617

Abstract

The response of a normally non-magnetic material to an external static magnetic field can be monitored by many different magnetic response functions. A general scheme to supply a corresponding theoretical description is presented that is based on the relativistic Korringa–Kohn–Rostoker Green function method of band structure calculations, and for that reason has many appealing features. First of all, it treats all spin as well as orbital contributions to the induced magnetization on the same footing, accounting in particular for all relativistic influences. Furthermore, it is extremely flexible and applicable in principle to any kind of system. Finally, a formulation for any response function can be worked out on this platform in a rather straightforward way. This is demonstrated together with corresponding applications for the magnetic form factor, the magnetic susceptibility and the Knight shift. In addition, a description of the so-called field-induced magnetic circular dichroism in x-ray absorption will be presented. In particular, it is shown that this new magneto-optical effect supplies a rather unique probe, giving information separately on the spin and orbital susceptibility in an element-resolved way.

1. Introduction

The investigation of the response of a material to an external magnetic field is one of the standard ways to get information on its electronic structure. There are many different experimental techniques available for that purpose that probe a corresponding response function. Without doubt, the most common one is the magnetic susceptibility that can be measured by various types of magnetic balance or magnetometer. For normally non-magnetic transition metal systems, that are the main issue of this contribution, one usually has to consider a spin as well as an orbital contribution. A consistent theoretical description of the Pauli spin susceptibility was presented by Gunnarsson [1] and Janak [2] that, in particular, accounted for the Stoner enhancement in a parameter-free way within the framework of spin density functional theory (SDFT). While expressions for the orbital contribution to the susceptibility were already worked out in the 1960s by Hebborn and Sondheimer [3] corresponding calculations were performed only later [4–6]. While most of this work was done using a conventional $\vec{k}$-space band structure method, Benkowitsch and Winter [5] used a real space method based on the

Green function technique. In particular, these authors derived consistent expressions for the conventional diamagnetic Langevin and Landau as well as paramagnetic (PM) Van Vleck contributions to the orbital susceptibility.

The influence of the scalar-relativistic mass–velocity and Darwin corrections as well as of the spin–orbit coupling on the spin susceptibility were investigated in the past by various groups [7–10]. Staunton and co-workers used the fully relativistic version of the Korringa–Kohn–Rostoker (KKR) Green function method of band structure calculation as a platform for this purpose and investigated a number of pure transition metals. For the orbital susceptibility relativistic influences have been investigated by Yasui and Shimizu [11], who gave an explicit expression for a spin–orbit induced spin–orbital cross contribution χ_{so} to the susceptibility.

The theoretical approaches mentioned so far are essentially based on a linear response formalism. Alternatively, one can explicitly add a Zeeman term accounting for an external magnetic field to the Hamiltonian within a self-consistent band structure calculation [12]. This approach automatically accounts for the Stoner enhancement when a coupling to the spin of the electrons is considered and SDFT is used as a formal platform. A Stoner-like enhancement of the orbital susceptibility has been investigated by Hjelm *et al* [13] by adding the coupling term $\mu_B l_z B_{ext}$ to the Hamiltonian that, in addition, included Brooks' orbital polarization (OP) term [14].

Obviously, the magnetic susceptibility is just one of the many response functions that represents the magnetization induced by an external field. Accordingly, the various approaches developed to calculate spin and orbital susceptibilities can in general be adopted to deal with the corresponding parts of other response functions as well. This was demonstrated for example by Oh *et al* [4] who calculated the various contributions to the induced magnetic form factor that can be deduced from neutron scattering experiments. This is a rather interesting quantity, because in an indirect way it gives—in contrast to the global susceptibility—information on the spatial distribution of the induced magnetization. For ordered compounds, one can often get this information even in an element-resolved way. This appealing feature is inherent in the Knight shift that is a measure for the induced hyperfine field at a nuclear site. Again, a corresponding theoretical description including in particular all orbital contributions was developed by Ebert *et al* [15] starting from the work of Benkowitsch and Winter [5].

While the Knight shift clearly supplies element-specific information if a multi-component system is investigated, it cannot be seen as a direct measure for the local or partial susceptibility because there is no strict one-to-one correspondence between both quantities. In contrast to this, one may use the induced circular magnetic dichroism in x-ray absorption (MCXD) to probe the partial susceptibility, as was suggested recently [16]. This new magnetic probe seems to be very promising because not only does it supply element-specific information but it also allows us to split the partial susceptibility into its spin and orbital part.

In the following a theoretical scheme is presented that is based on the KKR Green function method within the framework of SDFT. This approach allows us to deal with all mentioned response functions in a unified way. In particular, a fully relativistic formulation is used to account for all spin–orbit influences. This is indispensable in the case of the field-induced MCXD.

2. Theoretical framework

The most appropriate way to deal with magnetic response functions would be to use the linear response formalism to determine in a first step the electronic current density induced by an external magnetic field B_{ext}. In a second step, the various response functions of interest can be obtained from this. In fact, this was the approach used by Benkowitsch and Winter [5] and Ebert *et al* [15] to deal with the orbital susceptibility and Knight shift, respectively.

There are several reasons to proceed along these lines. First of all, a fully relativistic treatment of the problem uses the current density as the central electronic quantity. Accordingly, there is no need for a sometimes artificial separation into spin and orbital parts. This applies in particular when one is dealing with the influence of the electron–electron interaction that gives rise to Stoner-like enhancement effects. Concerning density functional theory, that is the conventional platform when dealing with the electronic structure of solids, this leads in a natural way to current density functional theory (CDFT) [17, 18]. Finally, one has to mention that the derivation of expressions for a magnetic response function starts in many cases from an expression involving the induced current density [5, 15].

Unfortunately, application of CDFT is connected with many technical and practical complications. In particular, a convenient and reliable parametrization of the exchange–correlation energy and the corresponding potential is not yet available. Accordingly, only very few applications of CDFT to the calculation of magnetic response functions can be found so far in the literature [19]. Because of this situation, the conventional approach is adopted in the following, i.e. in spite of the fully relativistic treatment of the electronic structure all calculations are performed in the framework of SDFT. To account nevertheless for an enhancement of orbital contributions to a response function, Brooks' OP scheme has been used.

The starting point of our approach is the linear response formalism formulated by means of the Green function technique. Representing the coupling to an external magnetic field by the perturbation Hamiltonian $\Delta\mathcal{H}$ the Green function G^B representing the electronic structure in the presence of the field can be expressed in term of the Green function G for the field-free case by the Dyson equation:

$$G^B = G + G\Delta\mathcal{H}G^B. \tag{1}$$

Restricting to corrections of G linear in $\Delta\mathcal{H}$ one has

$$G^B = G + G\Delta\mathcal{H}G. \tag{2}$$

With G^B available the expectation value of any observable A can be obtained from the expression

$$\langle\mathcal{A}\rangle = -\frac{1}{\pi}\,\mathrm{Im\,Trace}\;\mathcal{A}G^B \tag{3}$$

$$\langle\mathcal{A}\rangle = -\frac{1}{\pi}\,\mathrm{Im\,Trace}\;(\mathcal{A}G + \mathcal{A}G\Delta\mathcal{H}G) \tag{4}$$

with $\mathcal{A}$ the corresponding operator. If the expectation value of the observable vanishes for the field-free case, obviously only the second field-dependent term in equation (4) has to be considered.

Using the relativistic KKR band structure method the real space representation $G(\vec{r}, \vec{r}', E)$ of the Green function needed to use equation (4) can be written as [20]

$$G(\vec{r}, \vec{r}', E) = \sum_{\Lambda\Lambda'} Z^n_\Lambda(\vec{r}, E)\tau^{nn'}_{\Lambda\Lambda'}(E)Z^{n'\times}_{\Lambda'}(\vec{r}', E) - \sum_{\Lambda}[Z^n_\Lambda(\vec{r}, E)J^{n\times}_\Lambda(\vec{r}', E)\Theta(r' - r) + J^n_\Lambda(\vec{r}, E)Z^{n\times}_\Lambda(\vec{r}', E)\Theta(r - r')]\delta_{nn'}. \tag{5}$$

Here $\vec{r}(\vec{r}')$ is assumed to be within the atomic cell $n(n')$ and $\tau^{nn'}_{\Lambda\Lambda'}(E)$ is the scattering path operator with the combined index $\Lambda = (\kappa, \mu)$ standing for the spin–orbit and magnetic quantum numbers κ and μ, respectively. Finally, the four-component wavefunctions Z^n_Λ and J^n_Λ are the regular and irregular solutions, respectively, to the single-site Dirac equation for the atomic site n.

The perturbation $\Delta\mathcal{H}$ in equation (2) in general represents the coupling of the spin and orbital motion to the external magnetic field. In addition to the direct Zeeman term $\Delta\mathcal{H}^B$

it includes a term $\Delta\mathcal{H}^{\mathrm{xc}}$ that represents the modified electron–electron interaction due to the induced magnetization. Within plain SDFT this feed-back term is given by the change in the spin-dependent exchange–correlation potential due to the spin magnetization [1, 2]. Within a relativistic calculation the spin contribution to $\Delta\mathcal{H}$ may therefore be written as [9]

$$\Delta\mathcal{H}_{\mathrm{spin}}(\vec{r}) = \Delta\mathcal{H}^{B}_{\mathrm{spin}}(\vec{r}) + \Delta\mathcal{H}^{\mathrm{xc}}_{\mathrm{spin}}(\vec{r}) \tag{6}$$

$$\Delta\mathcal{H}_{\mathrm{spin}}(\vec{r}) = \beta\sigma_z\mu_{\mathrm{B}}B_{\mathrm{ext}} + \beta\sigma_z K^{\mathrm{xc},n}_{\mathrm{spin}}(\vec{r})\gamma^n(\vec{r})\chi^n_{\mathrm{spin}}\mu_{\mathrm{B}}B_{\mathrm{ext}}. \tag{7}$$

Here the usual assumption has been made that $\Delta\mathcal{H}^{\mathrm{xc}}_{\mathrm{spin}}$ depends linearly on the induced spin magnetization $m_{\mathrm{spin}}(\vec{r}) = \gamma^n(\vec{r})\chi^n_{\mathrm{spin}}B_{\mathrm{ext}}$ with the normalized spin density $\gamma^n(\vec{r})$, the local spin susceptibility χ^n_{spin} for site n and the corresponding interaction kernel $K^{\mathrm{xc},n}_{\mathrm{spin}}(\vec{r})$ [1]. To determine the unknown local susceptibility χ^n_{spin} the spin magnetization $m_{\mathrm{spin}}(\vec{r})$ is calculated using equation (4) together with the Green function G^B leading to the expression

$$m^n_{\mathrm{spin}}(\vec{r}) = -\frac{\mu_{\mathrm{B}}}{\pi}\,\mathrm{Im}\int^{E_{\mathrm{F}}}\mathrm{d}E\sum_{n'}\int_{\Omega^{n'}_{\mathrm{WS}}}\mathrm{d}^3r'\,\beta\sigma_z G(\vec{r},\vec{r}',E)$$
$$\times\,(\beta\sigma_z + \beta\sigma_z K^{\mathrm{xc},n}_{\mathrm{spin}}(\vec{r}')\gamma^{n'}(\vec{r}')\chi^{n'}_{\mathrm{spin}})B_{\mathrm{ext}}G(\vec{r}',\vec{r},E), \tag{8}$$

with $\vec{r}'$ restricted to the atomic cell n'.

Integrating $m^n_{\mathrm{spin}}(\vec{r})$ within cell n and dividing by the external field B_{ext} an implicit equation for the local spin susceptibilities $\chi^{n'}_{\mathrm{spin}}$ is obtained. For a pure, i.e. a one-component system, this results in the well-known expressions:

$$\chi_{\mathrm{spin}} = S\chi^0_{\mathrm{spin}} \tag{9}$$

$$\chi_{\mathrm{spin}} = \frac{1}{1 - I\chi^0_{\mathrm{spin}}}\chi^0_{\mathrm{spin}}, \tag{10}$$

where χ^0_{spin} is the bare Pauli spin susceptibility with the Stoner enhancement ignored and the Stoner exchange–correlation integral I. For more complex systems, the local susceptibility $\chi^{n'}_{\mathrm{spin}}$ can be obtained by solving a system of linear equations analogous to equation (8).

The expressions worked out by Benkowitsch and Winter [5] for the diamagnetic Langevin, Landau and PM Van Vleck contributions to the orbital susceptibility can be transferred straightforwardly to their proper relativistic counterparts. For the corresponding Van Vleck magnetization $m^n_{\mathrm{VV}}(\vec{r})$ one obtains an expression completely analogous to that given in equation (8), with the spin operator σ_z replaced by the z component of the orbital angular momentum operator l_z. Within a plain SDFT calculation there is no orbital interaction kernel and therefore the second term would vanish [5]. However, a treatment within CDFT would lead to a feed-back of the induced orbital magnetization and therefore to a Stoner-like enhancement of the orbital susceptibility in analogy to equation (10). This mechanism has been accounted for in the past in some few cases by formulating the corresponding interaction kernel $K^{\mathrm{xc},n}_{\mathrm{orb}}(\vec{r})$ by making use of Brooks' OP scheme [13, 14]. This approach has also been used here.

From equations (4) and (8) one can see that the Pauli spin susceptibility χ_{spin} is obtained from the expectation value $\langle\sigma_z\rangle$ that is non-zero because of the perturbation $\Delta\mathcal{H}_{\mathrm{spin}}$ that also involves the spin operator σ_z. In an analogous way, the Van Vleck susceptibility χ_{VV} is connected to $\langle l_z\rangle$ and the perturbation $\Delta\mathcal{H}_{\mathrm{orb}}$ that involves the angular momentum operator l_z. Within a non-relativistic calculation there would be no cross terms $\langle\sigma_z\rangle - \Delta\mathcal{H}_{\mathrm{orb}}$ and $\langle l_z\rangle - \Delta\mathcal{H}_{\mathrm{spin}}$ [5]. However, including the spin–orbit coupling when calculating the underlying electronic structure, corresponding small contributions χ_{so} and χ_{os} to the spin and orbital susceptibility, respectively, occur. If not otherwise noted these will be combined with the Pauli spin and Van Vleck orbital susceptibilities. In addition the diamagnetic Langevin and

Landau susceptibilities have to be considered in the following only in a few cases. For that reason the orbital susceptibility will be identified with its normally dominating Van Vleck part if not otherwise noted.

Having calculated the local spin and orbital susceptibilities $\chi^n_{\rm spin}$ and $\chi^n_{\rm VV}$, respectively, including the Stoner enhancement mechanism, any response function directly related to the corresponding magnetization can be calculated straightforwardly. This applies, for example, for the induced form factor $f(\vec{q})$ that depends on the scattering vector $\vec{q}$. Within the widely used dipole approximation the corresponding normalized spin and orbital contributions to $f(\vec{q})$ are given by [21]

$$f_{\rm spin}(\vec{q}) = \frac{1}{\chi_{\rm spin} B_{\rm ext}} \int_{\Omega_{\rm WS}} {\rm d}^3 r \; j_0(\vec{q}\cdot\vec{r}) m_{\rm spin}(\vec{r}) \tag{11}$$

$$f_{\rm orb}(\vec{q}) = \frac{1}{\chi_{\rm orb} B_{\rm ext}} \int_{\Omega_{\rm WS}} {\rm d}^3 r \; (j_0(\vec{q}\cdot\vec{r}) + j_2(\vec{q}\cdot\vec{r})) m_{\rm orb}(\vec{r}). \tag{12}$$

For a comparison with experimental data stemming from elastic neutron scattering measurements, the appropriate average has to be taken:

$$\bar{f}(\vec{q}) = \frac{f_{\rm spin}(\vec{q})\chi_{\rm spin} + f_{\rm orb}(\vec{q})\chi_{\rm orb}}{\chi_{\rm spin} + \chi_{\rm orb}}. \tag{13}$$

With $\chi^n_{\rm spin}$ and $\chi^n_{\rm orb}$ available, the Hamiltonian $\Delta\mathcal{H}_{\rm spin}$ in equation (7) and its orbital counterpart $\Delta\mathcal{H}_{\rm orb}$ are obviously completely fixed. This way, the Green function G^B in equation (2) is also completely specified and the expectation value of any observable may be obtained from equation (4). An example for this is the Knight shift, which is determined for example by NMR and is connected with the hyperfine interaction operator

$$\mathcal{H}_{\rm hf} = -\frac{1}{c}\vec{j}_{\rm el}\cdot\vec{\mu}_{\rm n}\times\vec{r}/r^3, \tag{14}$$

where $\vec{\mu}_{\rm n}$ is the nuclear moment and $\vec{j}_{\rm el} = -ec\vec{\alpha}$ is the electronic current density with $\vec{\alpha}$ the vector of Dirac matrices [22]. This leads for the Knight shift to the following expression:

$$K = -\frac{e}{\pi B_{\rm ext}} {\rm Im} \int^{E_{\rm F}} {\rm d}E \, \frac{(\vec{r}\times\vec{\alpha})_z}{r^3} G^B(\vec{r},\vec{r},E), \tag{15}$$

that obviously accounts properly for all enhancement effects via $\Delta\mathcal{H}_{\rm xc}$. Calculating the Knight shift as sketched above will always give the total shift. However, a decomposition into the conventional Fermi contact, spin–dipolar and orbital contributions is possible by applying a corresponding decomposition to the hyperfine Hamiltonian $\mathcal{H}_{\rm hf}$ [23]. An additional analysis of the results is possible by restricting the perturbation Hamiltonian $\Delta\mathcal{H}$ used to determine G^B to its spin part $\Delta\mathcal{H}_{\rm spin}$ or its orbital part $\Delta\mathcal{H}_{\rm orb}$, respectively. This way one can get, for example, the contribution to the Knight shift $K_{\rm VV}$, that is the counterpart to the Van Vleck susceptibility $\chi_{\rm VV}$.

Another way to monitor the induced magnetization is supplied by optical experiments. An example for this is the magneto-optical Kerr effect in the visible regime of light [24]. Unfortunately, the resulting Kerr spectra are quite complex and cannot be straightforwardly connected with the induced magnetization. In contrast to this situation, the induced MCXD gives access to the spin and orbital magnetic susceptibilities in an element-specific way [25]. To get a proper description of this new kind of experiment the x-ray absorption coefficient $\mu_\lambda(\omega)$ for radiation of energy $\hbar\omega$ and polarization λ is expressed by [26]

$$\mu_\lambda(\omega) \propto \sum_i \langle\Phi_i|X^\dagger_{\vec{q}\lambda} G^B(E) X_{\vec{q}\lambda}|\Phi_i\rangle \Theta(E-E_{\rm F}), \tag{16}$$

where $X_{\vec{q}\lambda}$ stands for the electron–photon interaction operator and i numbers the involved core states $|\Phi_i\rangle$ with energy E_i and the corresponding final state energy $E = E_i + \hbar\omega$.

Because the external magnetic field breaks the time reversal symmetry, a magnetic circular dichroism will be induced that can be expressed by the difference in absorption for left and right circularly polarized light:

$$\Delta\mu(\omega) = \mu_+(\omega) - \mu_-(\omega). \tag{17}$$

Performing measurements, for example at the $L_{2,3}$-edges of transition metals, the so-called sum rules [27–30] can be applied in the usual way giving access to the induced spin and orbital moment connected with the d electrons of the absorbing atom. The spin moment $\mu_{\rm spin}$ of course stems primarily from the Pauli spin susceptibility, while the orbital moment $\mu_{\rm orb}$ is connected to the Van Vleck orbital susceptibility. In both cases there are minor spin–orbital cross contributions that occur because of the presence of spin–orbit coupling (see above and [11]).

3. Induced spin and orbital magnetization

The central quantities supplied by the theoretical approach sketched above are the induced spin and orbital magnetizations, $m_{\rm spin}(\vec{r})$ and $m_{\rm orb}(\vec{r})$, respectively. For the corresponding r-dependent spin susceptibility $\chi_{\rm spin}(\vec{r}) = \gamma(\vec{r})\chi_{\rm spin}$ it is usually assumed that the normalized spin density $\gamma(\vec{r})$ is well represented by the square of the wavefunctions $|\psi(\vec{r}, E_{\rm F})|^2$ at the Fermi level. Corresponding results are shown for the spherically averaged spin susceptibility $\chi_{\rm spin}(r)$ of Nb in the top panel of figure 1. Obviously, $\chi_{\rm spin}(r)$ is dominated by the contributions of the 4d electrons and accordingly reflects the r dependence and nodal structure of the corresponding wavefunctions. In line with this one finds that $\chi_{\rm spin}(r)$ gets more localized if one goes along a transition metal row.

The approximation for the spatial variation of $\gamma(\vec{r})$ mentioned above can be avoided by solving equation (8) self-consistently for $m_{\rm spin}(\vec{r})$. In some cases, as for example for Pd, this may be important because $m_{\rm spin}(\vec{r})$ determines the Stoner exchange correlation integral and in that way the Stoner enhancement factor S.

Figure 1 shows that the r-dependent orbital Van Vleck susceptibility $m_{\rm VV}(\vec{r})$ may be quite different from its spin counterpart $m_{\rm spin}(\vec{r})$. The reason for this is that $m_{\rm spin}(\vec{r})$ is primarily determined by the change in population of states with spin up and spin down around the Fermi level and for that reason can be well approximated by the average squared wavefunction $|\psi(\vec{r}, E_{\rm F})|^2$. $m_{\rm VV}(\vec{r})$, on the other hand, is connected with the distortion of the wavefunctions due to the external field. For that reason, all states around the Fermi level contribute. As a consequence $m_{\rm VV}(\vec{r})$ does not change as strongly as $m_{\rm spin}(\vec{r})$ if one goes along a transition metal row.

As indicated above, the various response functions allow us to monitor the induced spin and orbital magnetizations in a more or less direct way. The susceptibility gives just a spatial average of the sum of spin and orbital contributions for a system. The Knight shift, on the other hand, primarily probes the nuclear near region and for that reason supplies element-specific information. The form factor, on the other hand, reflects the r dependence of $m_{\rm spin}(\vec{r})$ and $m_{\rm VV}(\vec{r})$ by its dependence on the scattering vector $\vec{q}$. However, in spite of the complementary information supplied by these response functions none of them allows us to separate the spin and orbital contributions to the induced magnetization in a direct way. For that reason the field induced MCXD mentioned above seems to be a promising new tool that is able to supply this information.

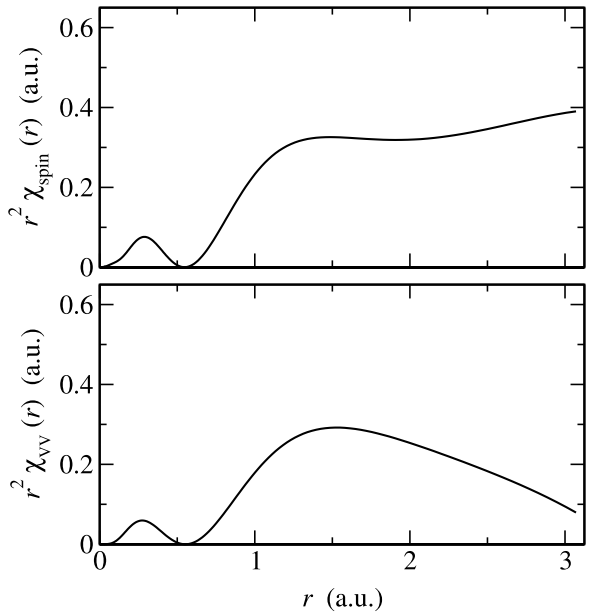

Figure 1. Spherically averaged spin and Van Vleck r-dependent susceptibilities $\chi_{\rm spin}(r)$ and $\chi_{\rm VV}(r)$, respectively, weighted with r^2 for Nb.

4. Magnetic susceptibility

The results obtained for the un-enhanced and enhanced Pauli spin susceptibility, $\chi^0_{\rm spin}$ and $\chi_{\rm spin}$, respectively, of 3d transition metals, using the relativistic formalism presented above, are rather close to those calculated before in a non-relativistic way [2]. Although the spin–orbit coupling has been included, $\chi^0_{\rm spin}$ is found to be essentially proportional to the density of states at the Fermi level $n(E_{\rm F})$. The Stoner enhancement factor S for the 3d transition metals lies in general between 1 and 2 (see figure 2). For Fe, Co and Ni the SDFT-based calculation correctly leads to a Stoner product $I\chi^0_{\rm spin}$ that is larger than 1, corresponding to a ferromagnetic instability. For that reason the enhanced spin susceptibility $\chi_{\rm spin}$ is not defined in this case.

In contrast to the spin susceptibility $\chi^0_{\rm spin}$ the orbital Van Vleck susceptibility $\chi^0_{\rm VV}$ varies quite smoothly along a transition metal row, as is shown in figure 3 for the 4d elements. The nearly parabolic variation of $\chi^0_{\rm VV}$ with the atomic number can be easily explained by the expression deduced via perturbation theory that leads to the expectation that, for a transition metal, $\chi^0_{\rm VV}$ should essentially be determined by the term $n_{\rm d}(10-n_{\rm d})/\Delta E$, with $n_{\rm d}$ the number of d electrons and ΔE the d-band width. In line with these considerations one finds that $\chi^0_{\rm VV}$ decreases when going from the 3d to the 4d and finally to the 5d transition metal row, because the d-band width ΔE increases along this sequence. In figure 3 the enhanced orbital susceptibility $\chi_{\rm VV}$ is also given that has been calculated using the OP formalism. As one notes, the enhancement is, in general, of the order of 10%. In particular one notes that this enhancement is much too small to give rise to a spontaneous magnetic ordering, as is the case for the spin susceptibility of Fe, Co and Ni.

The formalism presented in section 2 can be straightforwardly applied to disordered alloys [31]. Corresponding results for the alloy system Ag_xPt_{1-x} are shown in figure 4. As one can see, the calculations distinguish between the partial susceptibility of Ag and Pt, which turn out to be rather different. The two partial susceptibilities χ^α shown in figure 4 represent the

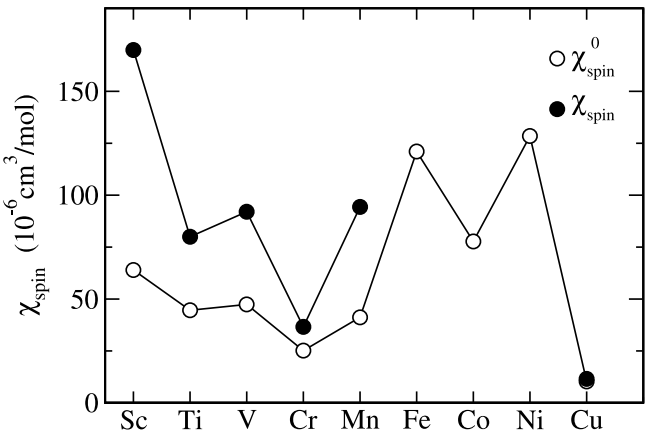

Figure 2. Un-enhanced and enhanced Pauli spin susceptibility χ^0_{spin} and χ_{spin}, respectively, of the 3d transition metals. Due to the ferromagnetic instability χ_{spin} is not defined for the PM state of Fe, Co and Ni.

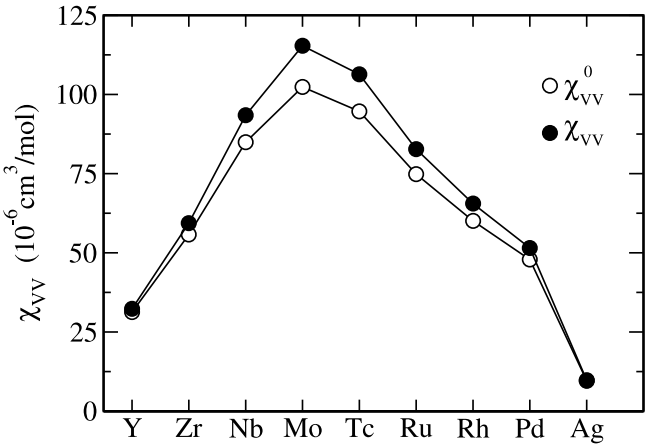

Figure 3. Un-enhanced and enhanced orbital Van Vleck susceptibility χ^0_{VV} and χ_{VV}, respectively, of the 4d transition metals. The Stoner-like enhancement has been treated using the OP formalism.

sum of the Pauli spin, the diamagnetic Langevin and the Van Vleck susceptibilities. Only the diamagnetic Landau susceptibility, which should be relatively small for this system, has been ignored. For Pt there is a nearly concentration-independent Van Vleck contribution to χ^{Pt}_{VV} that lies in the order of 40×10^{-6} emu mol^{-1}. The dominating contribution, however, stems from its spin part χ^{Pt}_{spin} that is connected with the d electrons. Obviously, this contribution is responsible for the pronounced concentration dependence of χ^{Pt} and with this also of the average susceptibility $\bar{\chi} = x_{Ag}\chi^{Ag} + x_{Pt}\chi^{Pt}$. The concentration dependence of χ^{Pt}_{spin} can be explained by the rapid decrease of the Pt density of states at the Fermi level $n^{Pt}(E_F)$ if Ag is added to Pt. This diminishes the un-enhanced partial spin susceptibility $\chi^{0,Pt}_{spin}$ accordingly, leading to an even more rapid decrease for the enhanced partial spin susceptibility χ^{Pt}_{spin}. In contrast to Pt there is only a minor variation of the partial susceptibility χ^{Ag} of Ag with concentration. In particular its spin part χ^{Ag}_{spin} is much smaller than that for Pt, in contrast to expectations based on a rigid band model.

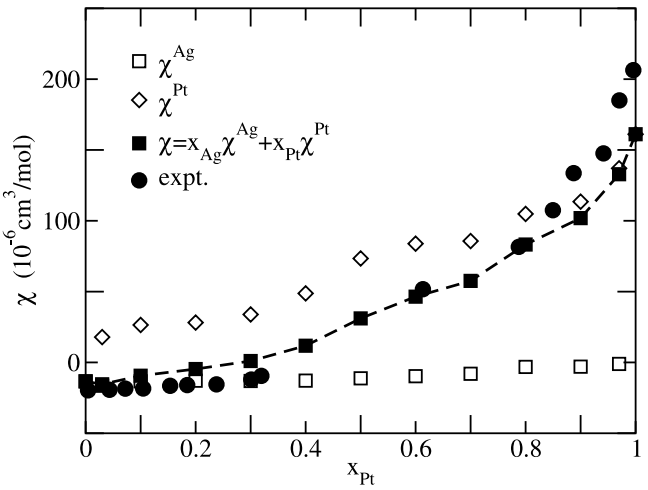

Figure 4. Calculated partial magnetic susceptibility for Ag and Pt in Ag_xPt_{1-x} as well as the total susceptibility as a function of the Ag concentration together with corresponding experimental data [32].

The resulting total average susceptibility $\bar{\chi}$ is compared in figure 4 with the corresponding experimental data. Corresponding measurements using a magnetometer or magnetic balance give only the total but not the partial susceptibilities. For that reason an interpretation of experimental data such as those shown in figure 4 is not straightforward. In fact, the rigid band model has frequently been used in the past in this situation, implying that the partial susceptibility of Ag and Pt in fcc-Ag_xPt_{1-x} should be the same. The calculations that give results in fairly good agreement with experiment definitely showed that this is not the case.

5. Knight shift

In contrast to a susceptibility measurement, element-specific information on the induced magnetization is obtained via NMR. Corresponding results for the Knight shift of Ag and Pt in the alloy system Ag_xPt_{1-x} are shown in figure 5. As can be seen, the Knight shift of Pt on the Pt-rich side is negative. The reason for this is the dominating core polarization contribution that has the same origin as its counterpart in ferromagnetic metals [33]. The high spin polarization of the d electrons, reflected by a large partial spin susceptibility $\chi^{\mathrm{Pt}}_{\mathrm{spin}}$, gives rise to a distortion of the core wavefunctions, leading this way to a hyperfine field that is proportional to the induced spin moment. Comparing the theoretical Knight shift of Pt with the experimental values one finds that the former ones are too small in magnitude. The reason for this discrepancy is that the core polarization mechanism is underestimated by plain SDFT-based calculations [33, 34]. In line with this one finds a fairly good agreement between theory and experiment for the Ag-rich side of the system. For this range of concentration the remaining contributions to the Knight shift—in particular that connected with the valence band s electrons—are dominating.

For Ag in Ag_xPt_{1-x} one also finds a negative Knight shift on the Pt-rich side of the system. Assuming a rigid-band behaviour one would ascribe this to a core-polarization contribution, as is present in the case of Pt. The results presented above for the partial spin susceptibility $\chi^{\mathrm{Ag}}_{\mathrm{spin}}$ of Ag, however, rule out this interpretation. This is also obvious from the calculated core

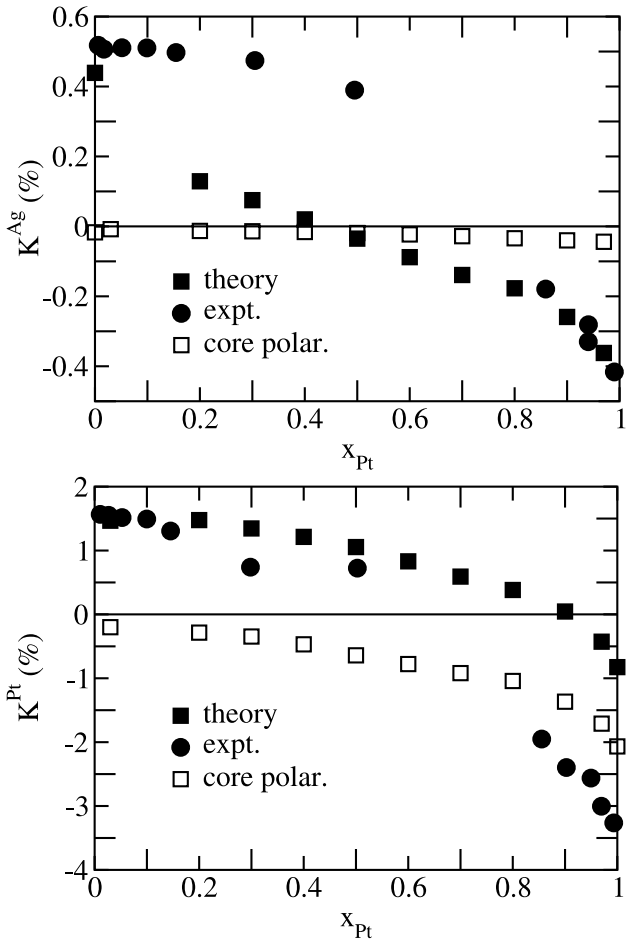

Figure 5. Knight shift K^{α} of Ag and Pt in Ag_xPt_{1-x} together with corresponding experimental data [32]. The open squares give the contribution to the theoretical Knight shift due to the core polarization mechanism.

polarization shift shown separately in figure 5. In contrast to Pt one finds that the negative Knight shift is connected with valence s electrons. Inspection of equation (15) shows that calculating the Knight shift one has to account for the perturbation due to the magnetic field not only at the central site but for the whole system, i.e. one has to perform the integration over the whole space. This implies that the strong spin polarization on the Pt atoms can have an impact at the Ag sites. This indeed gives rise to a transfer mechanism that leads to the negative Knight shift of Ag on the Pt-rich side [32, 35]. This obviously means that the Knight shift is not a local probe in a strict sense but it will always be influenced by the magnetic properties of the neighbouring atoms.

6. Magnetic form factor

Neutron scattering experiments have been done for quite a few pure transition metals and compounds to determine the induced magnetic form factor. To some extent, this work was

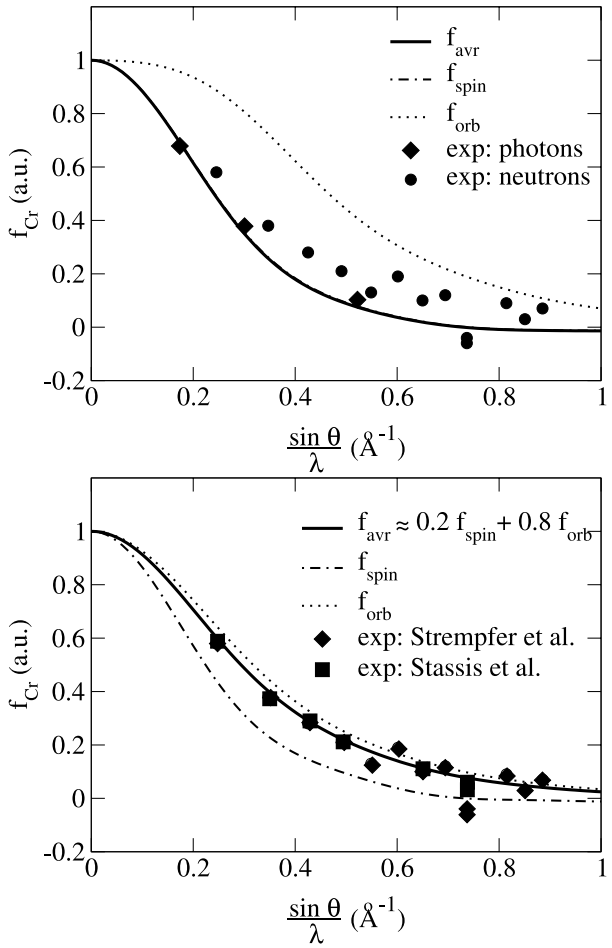

Figure 6. Top: spin, orbital and average magnetic form factor of AF-Cr. The full circles and diamonds give experimental data that stem from high-energy photon [36] and neutron [37] scattering experiments. Bottom: spin, orbital and average induced magnetic form factor of PM-Cr together with experimental data from neutron scattering experiments [38, 39].

motivated by the fact that the induced magnetic form factor reflects the degree of localization of the dominating d electrons. In other cases, the experiment was focused on the magnetic properties of the investigated system. An especially interesting case with respect to this is Cr that can be investigated in its antiferromagnetic (AF) ground state below the Neél temperature as well as in a PM state above it. A comparison of the various form factors is shown in figure 6 for the AF as well as the PM state. For the AF state, the neutron measurements were complemented recently by a non-resonant high energy x-ray scattering experiment, that probes only the spin part of the magnetic form factor [37]. From the finding that the results of both types of experiment hardly differ it was concluded that the permanent orbital magnetic moment in AF-Cr has to be very small. This could be confirmed by corresponding relativistic band structure calculations. The orbital magnetic form factor corresponding to the spin–orbit induced magnetization is shown separately in figure 6. Because the orbital moment is very small ($-0.0004\ \mu_B$), the total form factor is dominated by its spin part, which was found in very good agreement with the experimental data.

For the PM state of Cr, the situation is completely reversed. The induced magnetic form factor corresponding to the Van Vleck orbital susceptibility now contributes about 80% of the total magnetic form factor, as is shown in the lower part of figure 6. In addition, one notes that the orbital-induced form factor of PM-Cr does not decay as rapidly with the magnitude of the scattering vector $\vec{q}$ as its counterpart for AF-Cr. This indicates that the field-induced orbital magnetization in PM-Cr is more localized than the spin–orbit induced one in AF-Cr.

Finally, one should note that the calculated magnetic form factor of PM-Cr is in very good agreement with the experimental results that have been corrected for a minor diamagnetic contribution that is connected with the Langevin diamagnetism.

7. Field-induced magnetic circular x-ray dichroism

MCXD is now a standard tool to study spontaneously magnetized materials. In particular, it allows us to deduce from the corresponding dichroic spectra the spin and orbital magnetic moments of the absorbing atom by making use of the so-called sum rules. As could be demonstrated, for example, in the case of the Kerr effect, magneto-optical effects occur not only for spontaneously magnetized materials but also if the magnetization is imposed by an external magnetic field [24]. Accordingly, it is obvious that the MCXD should also be observable for non-magnetic solids in the presence of a magnetic field [16].

Figure 7 shows corresponding theoretical results obtained for the $M_{2,3}$ edge of fcc-Rh. The top panel shows the conventional x-ray absorption spectrum $\mu_{M_{2,3}}$ that is quite typical for an fcc transition metal. The lower panel gives the field-induced MCXD spectrum $\Delta\mu_{M_{2,3}}$ calculated for three different situations. The broken curve has been calculated assuming a coupling of the external field to the spin of the electrons only, i.e. $\Delta\mathcal{H}$ in equation (2) has been set to $\Delta\mathcal{H}_{\rm spin}$. The resulting MCXD spectrum $\Delta\mu_{M_{2,3}}$, i.e. the difference in absorption for left and right circularly polarized radiation, is very similar to that observed for Rh in the ferromagnetic alloy fcc-Co_xRh_{1-x} [40]. In this case there is only a minor spin–orbit induced orbital magnetic moment present for Rh, leading to a ratio of the MCXD amplitudes at the M_3 and M_2 edges of about -1:1. This is completely in line with the result obtained for $\Delta\mu_{M_{2,3}}$ in figure 7, for which only a minor orbital magnetization is induced via the spin–orbital cross mechanism.

If, on the other hand, $\Delta\mathcal{H}$ is set to $\Delta\mathcal{H}_{\rm orb}$, the ratio of the MCXD amplitudes is completely different, reflecting the strong induced orbital magnetization. Adding both curves together, one obtains the proper dichroic spectrum that now represents the combined spin and orbital magnetization. However, these two contributions can be decomposed by making use of the MCXD sum rules. In contrast to their conventional application to spontaneously magnetized solids, they now give the spin and orbital susceptibilities $\chi_{\rm spin}$ and $\chi_{\rm orb}$, respectively, as outlined in section 2. This procedure has been applied recently to induced MCXD spectra calculated for Pt in fcc-Ag_xPt_{1-x}, leading to results for $\chi^{\rm Pt}_{\rm spin}$ and $\chi^{\rm Pt}_{\rm orb}$ in very good agreement with those calculated directly [25].

8. Summary

A very flexible and powerful scheme to calculate magnetic response functions has been presented that makes use of the KKR Green function method of band structure calculation. Expressing the Green function of a system in the presence of a magnetic field in terms of an appropriate perturbation Hamiltonian and the Green function for the field-free case, the expectation value for any observable can be obtained straightforwardly. Corresponding

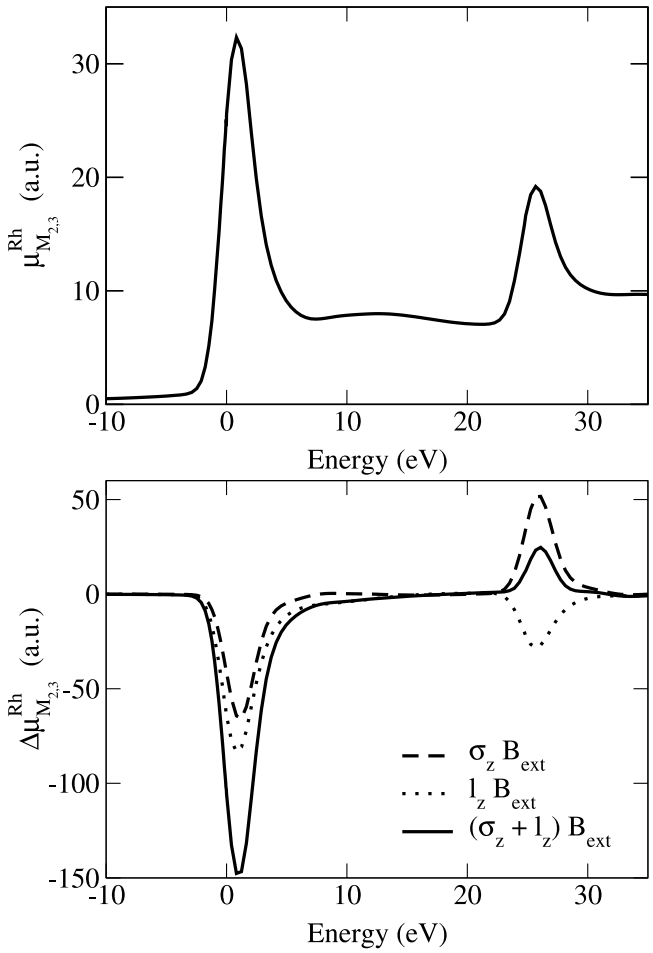

Figure 7. Absorption coefficient $\mu_{M_{2,3}}$ and induced MCXD spectrum $\Delta\mu_{M_{2,3}}$ for the $M_{2,3}$ edges of Rh in fcc-Rh.

expressions and results are presented for the spin and orbital magnetic susceptibilities which, in particular, include corrections due to the Stoner enhancement. This also applies for the Knight shift data presented for Ag_xPt_{1-x}. These results clearly demonstrate the possible occurrence of a negative Knight shift due to neighbouring atoms with a large local spin susceptibility. For AF- as well as PM-Cr the corresponding form factors were discussed in detail. Comparison of the orbital form factors clearly showed that the spin–orbit and field-induced orbital magnetization in AF- and PM-Cr, respectively, have a rather different spatial distribution. Finally, first results for the field-induced MCXD have been presented that demonstrate that this might be a very helpful analytical tool in the future that gives access to the spin and orbital susceptibility separately in an element-resolved way.

Acknowledgment

This work was funded by the DFG (Deutsche Forschungsgemeinschaft).

References

[1] Gunnarsson O 1976 *J. Phys. F: Met. Phys.* **6** 587
[2] Janak J F 1977 *Phys. Rev.* B **16** 255
[3] Hebborn J E and Sondheimer E H 1960 *J. Phys. Chem. Solids* **13** 105
[4] Oh K H, Harmon B N, Liu S H and Sinha S K 1976 *Phys. Rev.* B **14** 1283
[5] Benkowitsch J and Winter 1983 *J. Phys. F: Met. Phys.* **13** 991
[6] Yasui M and Shimizu M 1979 *J. Phys. F: Met. Phys.* **9** 1653
[7] Koelling D D and MacDonald A H 1983 *Relativistic Effects in Atoms, Molecules and Solids* ed G L Malli (New York: Plenum) p 227
[8] MacDonald A H 1982 *J. Phys. F: Met. Phys.* **12** 2579
[9] Staunton J B 1982 *PhD Thesis* University of Bristol
[10] Matsumoto M, Staunton J B and Strange P 1990 *J. Phys.: Condens. Matter* **2** 8365
[11] Yasui M and Shimizu M 1985 *J. Phys. F: Met. Phys.* **15** 2365
[12] Gräf P, Ebert H, Akai H and Voitländer J 1993 *Hyperfine Interact.* **78** 1011
[13] Hjelm A *et al* 1995 *Int. J. Mod. Phys.* B **9** 2735
[14] Brooks M S S 1985 *Physica* B **130** 6
[15] Ebert H, Winter H and Voitländer J 1986 *J. Phys. F: Met. Phys.* **16** 1133
[16] Ebert H, Deng M and Freyer H 2001 *Field Induced Magnetic Circular Dichroism in Paramagnetic Solids (Springer Lecture Notes in Physics vol 565)* ed J-P Kappler (Berlin: Springer) p 343
[17] Rajagopal A K and Callaway J 1973 *Phys. Rev.* B **7** 1912
[18] Vignale G and Rasolt M 1987 *Phys. Rev. Lett.* **59** 2360
[19] Colwell S M and Handy N C 1994 *Chem. Phys. Lett.* **217** 271
[20] Staunton J B, Gyorffy B L and Weinberger P 1980 *J. Phys. F: Met. Phys.* **10** 2665
[21] Brooks M S S, Eriksson O, Severin L and Johansson B 1993 *Physica* B **192** 39
[22] Rose M E 1961 *Relativistic Electron Theory* (New York: Wiley)
[23] Battocletti M and Ebert H 2001 *Phys. Rev.* B **64** 094417
[24] Yaresko A N *et al* 1998 *Phys. Rev.* B **58** 7648
[25] Ebert H and Mankovskyy S 2002 unpublished
[26] Ebert H 1996 *Rep. Prog. Phys.* **59** 1665
[27] Wienke R, Schütz G and Ebert H 1991 *J. Appl. Phys.* **69** 6147
[28] Thole B T, Carra P, Sette F and van der Laan G 1992 *Phys. Rev. Lett.* **68** 1943
[29] Schütz G, Knülle M and Ebert H 1993 *Phys. Scr.* T **49** 302
[30] Carra P, Thole B T, Altarelli M and Wang X 1993 *Phys. Rev. Lett.* **70** 694
[31] Deng M, Freyer H and Ebert H 2000 *Solid State Commun.* **114** 365
[32] Ebert H, Abart J and Voitländer J 1984 *J. Phys. F: Met. Phys.* **14** 749
[33] Ebert H, Strange P and Gyorffy B L 1988 *J. Phys. F: Met. Phys.* **18** L135
[34] Akai H and Kotani T 1999 *Hyperfine Interact.* **120/121** 3
[35] Ebert H and Winter H 1987 *Solid State Commun.* **63** 899
[36] Moon R M, Koehler W C and Tergo A L 1966 *J. Appl. Phys.* **37** 1036
[37] Strempfer J *et al* 2000 *Eur. Phys. J.* B **14** 63
[38] Stassis C, Kline G R and Sinha S K 1975 *Phys. Rev.* B **11** 2171
[39] Strempfer J *et al* 1999 *Physica* B **267/268** 56
[40] Harp G R, Parkin S S P, O'Brien W L and Tonner B P 1995 *Phys. Rev.* B **51** 12037